

FATIGUE ANALYSIS ON FLAX-EPOXY COMPOSITES: INSIGHTS AND IMPLICATIONS

ANDREA PAGLIARO*, LORENZO CAGNETTA

Università degli Studi Niccolò Cusano, Roma, Via Don Carlo Gnocchi 3, Italy

* corresponding author: andrea.pagliaro@unicusano.it

ABSTRACT. This study investigates the performance of flax fiber and epoxy resin composites, focusing on fatigue testing, which is scarcely reported in the literature. Fatigue behavior is evaluated under full reverse bending loading conditions: $R = -1$. Apart of the definition of the classic S-N curve, the analysis deeply investigated the evolution of the hysteresis leaf generated during each cycle over the entire fatigue life. This approach allows evaluating interesting parameters such as the evolution of the loss factor and the apparent modulus over life, being these informations fundamental for practical application of natural-fiber composites in engineering applications.

KEYWORDS: Bio-based composite, flax, fatigue, reverse bending, hysteresis.

1. INTRODUCTION

This study investigates the fatigue behavior of composite materials reinforced with natural fibers, addressing a critical yet under-explored aspect of materials science. Composite materials, recognized for their versatility and strength, are increasingly being reinforced with natural fibers to enhance their environmental sustainability and mechanical properties. Existing literature presents numerous studies on tensile and cyclic tensile testing of natural-fiber composites, offering valuable insights into their initial mechanical performance and failure modes under static and dynamic loads.

Specifically, the research conducted by Charlet et al. [1] focuses on tensile testing of flax composites with an epoxy resin matrix, revealing nonlinear behavior. Additionally, the study by Mahboob et al. [2] expands on tensile testing by incorporating an analysis under increasing cyclic loads until failure in both tension and compression, elucidating the damage evolution in the material. Further contributions by Giuliani et al. [3, 4] investigate both the material's nonlinearity and the influence of strain rate. An additional noteworthy study by Giuliani et al. [5] explores the effects of creep and stress relaxation phenomena. The findings emphasize the significance of viscoelastic (VE), viscoplastic, and pseudo-plastic components in the mechanical response of natural fiber-reinforced polymers (NFRPs), in contrast to traditional composites (such as glass and carbon fiber-reinforced polymers), whose responses are typically approximated as linear-elastic.

Nevertheless, a limited number of studies have addressed the evolution of material behavior under fatigue, a critical consideration for long-term structural applications [6, 7]. Fatigue behavior is pivotal as it determines the durability and reliability of materials subjected to repeated loading and unloading cycles over extended periods. Understanding the behavior of these composites under such conditions is essen-

tial for their application in the automotive, aerospace, and civil engineering sectors, where materials are frequently exposed to fluctuating stresses.

In addition to conventional analyses, such as stress-strain response and failure modes, this research examines parameters like the apparent modulus and the loss factor throughout the material's lifespan. The apparent modulus provides insights into the stiffness degradation of the material under cyclic loading, indicating changes in the material's ability to withstand deformation over time. The investigation of the loss factor is particularly significant due to the superior damping properties exhibited by natural fibers compared to traditional composites. Damping properties are crucial for reducing vibrations and enhancing the comfort and safety of structures and vehicles. The superior damping capacity of natural fibers, like flax fibers used in this study, allows composites reinforced with these fibers to absorb and dissipate more energy, resulting in reduced noise and vibration.

By exploring these parameters, this study aims to provide a comprehensive understanding of the fatigue behavior of natural fiber-reinforced composites. This understanding will facilitate the prediction of the lifespan and performance of these materials and optimize their design for specific applications where long-term durability and energy absorption are paramount.

2. MATERIALS AND METHODS

The material under investigation is a natural fiber composite. Specifically, pre-preg flax fibers arranged in a fully unidirectional manner and embedded in an epoxy resin matrix were utilized. The laminate has been cured in autoclave stacking 13 layers of unidirectional (UD) pre-preg with 50 % of fiber resin content, resulting in a final cured thickness of 2.75 mm. All the process parameters are reported in Table 1.

Conducting fatigue tests under full reverse loading conditions ($R = -1$) using axial tension and compres-

Temp.	Pres.	Time	Rate
130 °C	5 bar	1 h	2 °C · min ⁻¹

TABLE 1. Autoclave curing process parameters.

sion would have posed substantial challenges due to buckling phenomena occurring during the compression phase. Consequently, an alternative approach was necessary, leading to the implementation of bending tests.

Reverse bending fatigue tests have been conducted on specimens 100 mm long, 10 mm wide, and 2.75 mm thick. Such dimensions do not correspond to any standard, as full-reverse-bending tests are not common in the literature due to the non-trivial loading condition.

We have been able to perform these tests thanks to dedicated patented jigs allowing to apply pure reverse bending loads using traditional universal testing machine originally meant for axial testing [8] reported in Figure 1.

All the specimens have been cut out of a single plate through CNC routing utilizing a diamond carbide bit. Overall, 11 specimens have been tested under stress-controlled fatigue loading with a 2 Hz sinusoidal load history for varying stress ratios, imposing as run-out value a cycle count of 2 million cycles.

The frequency was carefully chosen to be low enough to avoid self-heating of the material and to prevent undesirable effects from strain rate sensitivity, which this visco-elastoplastic material is particularly prone to. Conversely, it was selected to be high enough to reduce the typically long durations associated with fatigue testing.

Apart the definition of the mere SN-curve, some parameters of interest have been taken into account by analysing in detail the hysteresis cycles obtained at selected load cycles. More in detail, over the entire fatigue life we recorded the hysteresis cycles over the first 200 cycles and then on a logarithmic base acquiring 10 cycles per logarithmic decade, plus the last 200 cycles prior to the final failure.

The parameters of interest in this study pertain to the hysteresis loop characteristic of viscous materials subjected to cyclic loading, as depicted in Figure 2. The upper image illustrates the loading and unloading phases of a single cycle, for instance, related to a load history with a stress ratio $R = 0.1$ defined as the ratio σ_{\min} to σ_{\max} (Eq. 7). Additionally, the first parameter of interest is here defined as the apparent modulus E_a which, at each cycle, is calculated as the ratio $\Delta\sigma$ to $\Delta\varepsilon$ (Eq. 8), being $\Delta\sigma$ the difference between the maximum (σ_{\max}) and the minimum (σ_{\min}) flexural stress, and $\Delta\varepsilon$ the difference between the maximum and the minimum strains attained on the outer layer. Please note that stress and the strain have been estimated from the force-displacement data acquired by the load cell following Eq. 1 and 2, respectively.

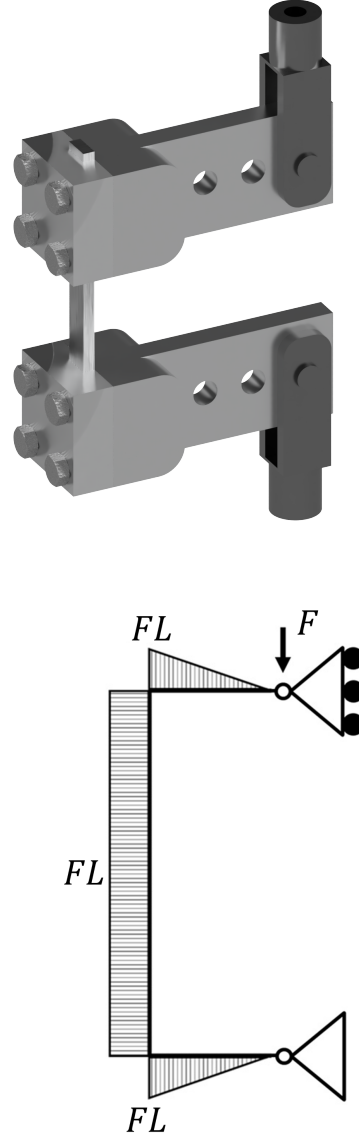


FIGURE 1. Detail of the dedicated jigs utilized for the fatigue tests (top), and schematic diagram of the applied forces and the induced internal moments (bottom).

$$\sigma(t) = \frac{6F(t)L}{w \cdot t^2} \quad (1)$$

$$\varepsilon(t) = \frac{h(t) - h_0}{h_0}; \quad (2)$$

being F the force read by the load cell, L the distance from the load axis to the neutral axis of the specimen, w the specimen's width, t the specimen's thickness, h the deformed outer length and h_0 the undeformed length of the neutral axis corresponding to the useful section of the sample between the gripping points.

To determine the deformed outer length $h(t)$, data from the testing machine were utilized. Specifically, referring to Figure 3, the axial displacement of the movable piston in the direction of the force F , defined

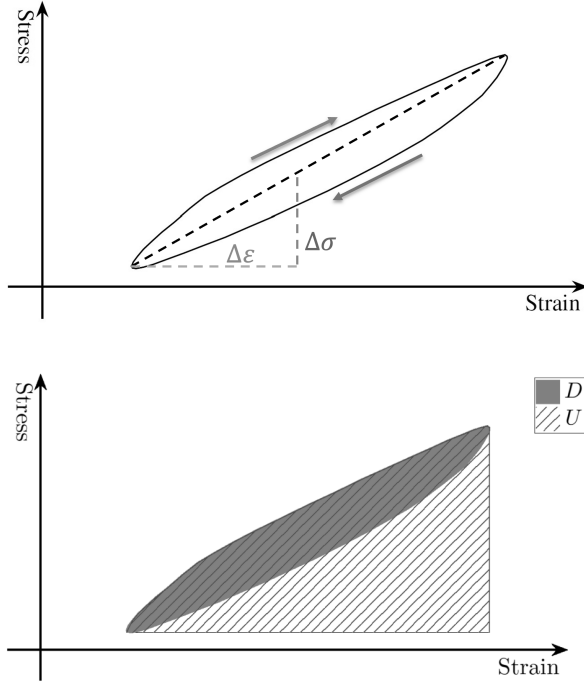


FIGURE 2. Parameters of interest: Apparent modulus (top) and energy lost in a single hysteresis cycle (bottom).

as $Z(t)$, was considered. For symmetry reasons, only half of the sample was analyzed, as shown in Eq. 3.

By considering the displacement over time and the fixed dimension L , the angle at the specimen's end can be easily calculated using the relation in Eq. 4. Subsequently, the radius of curvature with respect to the sample's neutral axis is calculated using Eq. 5, thus providing the curvature of the neutral axis over time. The evolution of the strain on the outer surface is finally computed as Eq. 6.

$$z(t) = \frac{Z(t)}{2} \quad (3)$$

$$\alpha(t) = \arcsin \frac{z(t)}{L} \quad (4)$$

$$r(t) = \frac{z_0}{\alpha(t)} \quad (5)$$

$$\varepsilon(t) = \frac{1}{r(t)} \cdot \frac{t}{2} \quad (6)$$

The second parameter of interest, referring to the lower image in Figure 2, is the loss factor η . It is defined by Macioce et al. [9] as the ratio of the energy dissipated during the cycle D to the energy stored during the loading phase U , scaled by 2π .

Additionally, this factor corresponds to twice the damping coefficient ξ , as reported in Eq. 9.

$$R = \frac{\sigma_{\min}}{\sigma_{\max}} \quad (7)$$

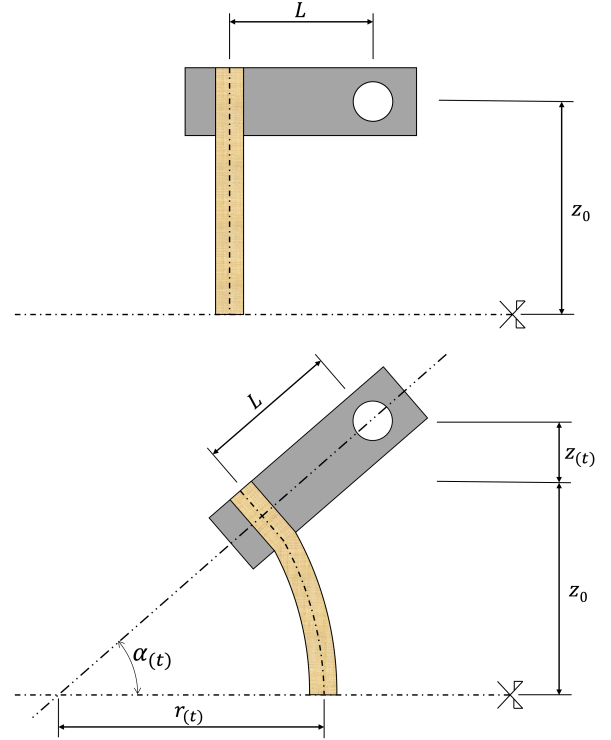


FIGURE 3. Neutral position (top), and deformed position which introduce bending moment on the specimen (bottom).

$$E_a = \frac{\Delta\sigma}{\Delta\varepsilon} \quad (8)$$

$$\eta = \frac{D}{2\pi U} = 2\xi \quad (9)$$

3. RESULTS

The initial results are derived from the standard SN curve for fatigue tests, reported in Figure 4. It effectively characterizes the material's performance up to a maximum of $2 \cdot 10^6$ cycles. To get some more insights apart the SN curve, emphasis is placed on the analysis of the evolution of the hysteresis cycles over the fatigue life.

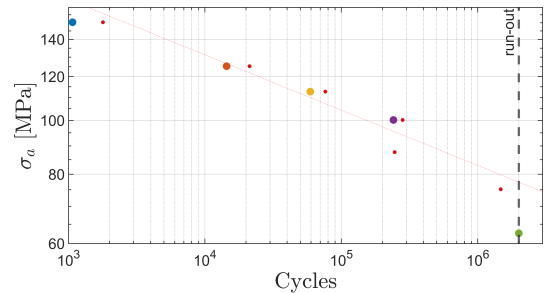


FIGURE 4. Experimental results (solid marks) and derived S-N curve (dashed line).

Two examples of the hysteresis cycles evolution over life are reported in Figure 5. The upper graph reports

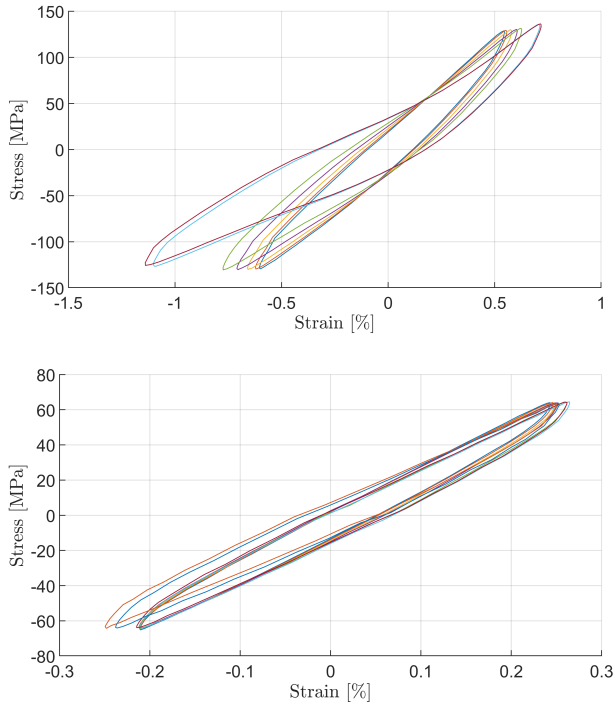


FIGURE 5. Evolution of the hysteresis cycles over life for the specimen failed at 14500 cycles (top) and for the infinite life case (bottom).

the case of a short lifespan, which associates to a high loading condition. More precisely, it corresponds to the third marker from the left in Figure 4, which failed at approximately 14 500 cycles. It is evident that over cycles, the hysteresis leaf progresses towards higher strain values in both tension and compression. Such behavior suggests a stiffness decrease over life which, due to the $R = -1$ condition, should be ascribed to progressive internal damage, as better detailed later on.

The lower graph in Figure 5 illustrates the evolution of the hysteresis leaf for the longest-lived case examined in this study. This corresponds to the case achieving infinite life (last large marker on the right in Figure 4). It is evident that there has been a noticeably limited evolution of strain, albeit showing a slight progression following a trend similar to the previous case.

The continuous evolution of the hysteresis cycles over life is reflected in the concurrent evolution of the pre-defined key parameters. To analyze the evolution of the parameters with increasing fatigue cycles, five points were selected from the S-N curve, which are highlighted in Figure 4 with larger markers. To each one of these five points, the evolution of the hysteresis cycles have been analyzed over the entire fatigue life, allowing to derive the evolution of the parameters of interest: the apparent modulus E_a and the loss factor η , whose evolution are presented in Figure 6.

Significantly, the trend is notably influenced by the load intensity under full reverse bending conditions. Specifically, there is an approximate 10 GPa variation

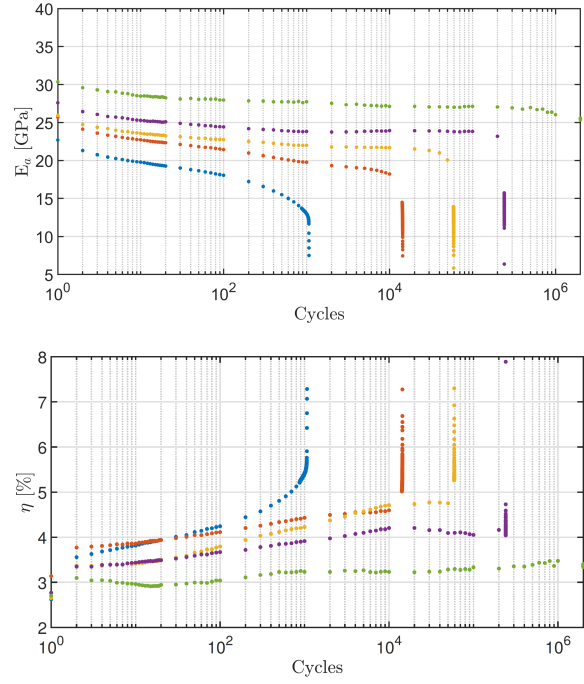


FIGURE 6. Evolution of the apparent elastic modulus (top) and damping ratio (bottom) over life for selected specimens at varying fatigue lives.

in apparent modulus between the shortest lifespan case, depicted by the lowest curve on the graph, and the infinite lifespan case, represented by the uppermost curve. The highest apparent modulus value, initialing attaining 31 GPa and consistently exceeding 27 GPa over the entire life, is observed under infinite lifespan conditions, while the lower apparent modulus, initially attaining 23 GPa and rapidly dropping below 15 GPa, is attained by the highly-loaded specimen. For all the loading conditions the behavior of the apparent modulus shows a continuous decline until reaching the latter part of its life, where it undergoes a sudden drop just before failure.

The large influence of the loading condition on the initial value of the apparent modulus should be ascribed to the highly nonlinear behavior of natural-fiber composites, which shows an almost bi-linear stress-strain curve [5], hence the modulus at the lower loads is much higher than the one at the larger loads.

Conversely, there is an inverse trend observed with respect to the loss factor. In this instance, all scenarios demonstrate an increase throughout their lifespan, contrasting with the apparent modulus, until showing a sharp increase just before failure. The variation in the loss factor is approximately 1 % across different lifespans. The most favorable outcome in terms of the loss factor occurs for the shortest lifespan, consistently exceeding 4 %.

A highly significant result arises from the damping factor values. In all cases, values exceeding 3 % are observed throughout the fatigue life, indicating the persistence or increase of this property with cycle accumulation.

4. CONCLUSIONS

This study conducted a comprehensive analysis of the hysteresis loop to define two critical parameters that facilitate the evaluation of a material's performance throughout its fatigue life: the apparent modulus (E_a) and the damping capacity, closely related to the loss factor (η).

The apparent modulus (E_a) is crucial for understanding the evolution of a material's stiffness as it endures over the lifespan. This parameter highlights the relationship between load intensity and evolution of the stiffness over life. As the number of cycles increases, changes in the material's stiffness are quantified through the apparent modulus. This measure is essential for predicting the material's performance and lifespan under cyclic loading conditions, providing insights into how stiffness degrades or evolves over time.

The second parameter: the damping capacity, is intrinsically linked to the loss factor (η). This parameter evaluates the material's ability to dissipate energy, a critical aspect of performance under cyclic loads. The study shows that η values never fall below 3%, indicating consistently good damping capacity. This finding is significant as it demonstrates the material's reliability in energy dissipation even under extensive cyclic loading. Maintaining a minimum loss factor of 3% suggests robust damping capacity, making the material suitable for applications requiring effective energy dissipation.

In conclusion, this study offers significant insights into the fatigue behavior of materials through detailed analysis of the apparent modulus and loss factor. By addressing the evolution of stiffness and damping capacity during fatigue life, the research fills a notable gap in the existing literature. These findings are particularly valuable for the design and optimization of components or structures made of natural fiber composites. Understanding the behavior of these materials under cyclic loading conditions can lead to improved performance and longer lifespans for final products. This research advances knowledge in the field and provides practical guidelines for engineers and designers working with natural fiber composites. The comprehensive evaluation of the hysteresis loop and defined

parameters serves as a foundation for future studies aiming to enhance material performance in fatigue applications.

REFERENCES

- [1] K. Charlet, S. Eve, J. P. Jernot, et al. Tensile deformation of a flax fiber. *Procedia Engineering* **1**(1):233–236, 2009. <https://doi.org/10.1016/j.proeng.2009.06.055>
- [2] Z. Mahboob, I. El Sawi, R. Zdero, et al. Tensile and compressive damaged response in Flax fibre reinforced epoxy composites. *Composites Part A: Applied Science and Manufacturing* **92**:118–133, 2017. <https://doi.org/10.1016/j.compositesa.2016.11.007>
- [3] P. M. Giuliani, O. Giannini, R. Panciroli. Viscoelastic experimental characterization of flax/epoxy composites. *Procedia Structural Integrity* **12**:296–303, 2018. <https://doi.org/10.1016/j.prostr.2018.11.086>
- [4] P. M. Giuliani, O. Giannini, R. Panciroli. Characterizing flax fiber reinforced bio-composites under monotonic and cyclic tensile loading. *Composite Structures* **280**:114803, 2022. <https://doi.org/10.1016/j.compstruct.2021.114803>
- [5] P. M. Giuliani, O. Giannini, R. Panciroli. Creep and stress relaxation of unidirectional flax fiber reinforced laminates. *Composite Structures* **310**:116755, 2023. <https://doi.org/10.1016/j.compstruct.2023.116755>
- [6] Z. Mahboob, H. Bougherara. Fatigue of flax-epoxy and other plant fibre composites: Critical review and analysis. *Composites Part A: Applied Science and Manufacturing* **109**:440–462, 2018. <https://doi.org/10.1016/j.compositesa.2018.03.034>
- [7] F. Bensadoun, K. A. M. Vallons, L. B. Lessard, et al. Fatigue behaviour assessment of flax-epoxy composites. *Composites Part A: Applied Science and Manufacturing* **82**:253–266, 2016. <https://doi.org/10.1016/j.compositesa.2015.11.003>
- [8] G. S. Ponticelli, R. Panciroli, S. Venettacci, et al. Experimental investigation on the fatigue behavior of laser powder bed fused 316L stainless steel. *CIRP Journal of Manufacturing Science and Technology* **38**:787–800, 2022. <https://doi.org/10.1016/j.cirpj.2022.07.007>
- [9] P. Macioce. Viscoelastic damping 101. *Sound and Vibration* **1**:10–12, 2003.